

January 2006

On correlations and discreteness in non-linear QCD evolution

N. Armesto¹ and J. G. Milhano^{2,3}

¹ *Departamento de Física de Partículas and IGFAE,
Universidade de Santiago de Compostela, 15782 Santiago de Compostela, Spain*

² *CENTRA, Instituto Superior Técnico (IST),
Av. Rovisco Pais, P-1049-001 Lisboa, Portugal*

³ *Departamento de Física, FCT, Universidade do Algarve,
P-8000-117 Faro, Portugal*

We consider modifications of the standard non-linear QCD evolution in an attempt to account for some of the missing ingredients discussed recently, such as correlations, discreteness in gluon emission and Pomeron loops. The evolution is numerically performed using the Balitsky-Kovchegov equation on individual configurations defined by a given initial value of the saturation scale, for reduced rapidities $y = (\alpha_s N_c/\pi) Y < 10$. We consider the effects of averaging over configurations as a way to implement correlations, using two types of Gaussian averaging around a mean saturation scale. Further, we heuristically mimic discreteness in gluon emission by considering a modified evolution in which the tails of the gluon distributions are cut-off. The approach to scaling and the behavior of the saturation scale with rapidity in these two modified evolutions are studied and compared with the standard mean-field results. For the large but finite values of rapidity explored, no strong quantitative difference in scaling for transverse momenta around the saturation scale is observed. At larger transverse momenta, the influence of the modifications in the evolution seems most noticeable in the first steps of the evolution. No influence on the rapidity behavior of the saturation scale due to the averaging procedure is found. In the cut-off evolution the rapidity evolution of the saturation scale strongly depends on the value of the cut-off. Our results stress the need to go beyond simple modifications of evolution by developing proper theoretical tools that implement such recently discussed ingredients.

1 Introduction

The B-JIMWLK¹ equations, derived over the last decade as a result of the concerted effort of several groups [1–15], build upon the original ideas on gluon saturation set out in [16] to provide the contemporary description of the evolution of QCD scattering amplitudes at high energy. Unfortunately, these are complicated equations and their complete solution is unknown. A combination of numerical [17–25] and analytical [26–32] studies has established the asymptotic properties of the B-JIMWLK equations. Most of these studies have focused on the mean field limit of the equations, where the B-JIMWLK set reduces to a single closed equation [12,33] - the Balitsky-Kovchegov (BK) equation. Nevertheless, the results obtained for the BK equation are known to deviate at the most $\sim 10\%$ from those obtained numerically for the full B-JIMWLK [25].

In obtaining this set of equations, the gluonic density in the target was assumed to be large, and the projectile was taken as a dilute object. The strict validity of the resulting evolution scheme is, therefore, restricted to this physical domain. Further, it has become clear that the physical region of interest - i.e. that within reach of accelerators that are currently operating and those that will be operational in the near future - lies within the pre-asymptotic region of the evolution and that in this region the evolution is dominated by the, as yet unknown, initial conditions [24,34,35].

In the last year, there has been a spurt of activity in this domain triggered by the crucial observation that important effects for the evolution in the pre-asymptotic region are absent from the currently available evolution scheme [36–39]. These new contributions stem from the understanding of the importance of gluon fluctuations and have been variably referred to as 'Pomeron loops' [39–42], 'fluctuations' [38] or 'wave function saturation effects'. These effects will yield both important contributions in the intermediate pre-asymptotic regime, and changes in less inclusive observables in the saturated regime.

A particularly important development has been the finding of a duality transformation connecting the high and low density regimes [43,44]. This duality places strict constraints on the form of the evolution kernel in the intermediate region. Nonetheless, the evolution in this intermediate domain is not completely understood.

¹Balitsky–Jalilian–Marian–Iancu–McLerran–Weigert–Leonidov–Kovner.

At this stage, and while efforts towards the derivation of the complete evolution take place, it appears possible to attempt to implement some of the effects as effective modifications of the BK equation.

In this paper, we assess the impact of some of the proposed new contributions. In particular, we address the effect of correlations by introducing an averaging procedure for the initial conditions for the evolution. Further, we model possible effects due to the discreteness in gluon emission by considering the BK evolution of gluon distributions with cut-off tails.

The paper is organized as follows. In Section 2 we outline the numerical method used to implement the BK equation, and the procedures adopted to introduce modifications in the evolution that can mimic the effects of correlations and gluon discreteness. Our results are presented in Section 3 and discussed in Section 4.

2 Numerical method

Non-linear QCD evolution is implemented using the BK equation [33] in momentum space in the local approximation (i.e. neglecting the impact parameter dependence). This approximation should be valid for a large nucleus in the region far from its periphery. The evolved object is the unintegrated gluon distribution $\phi(k, b) \equiv \phi(k)$ with k the transverse momentum, b the impact parameter and where the dependence on rapidity Y is implicitly understood. The unintegrated gluon distribution is related to the scattering probability of a $q\bar{q}$ dipole of transverse size r on a hadronic target, $N(r, b) \equiv N(r)$, through

$$\phi(k) = \int \frac{d^2 r}{2\pi r^2} e^{-ik \cdot r} N(r). \quad (1)$$

For the azimuthally independent piece of the solution, which gives the dominant contribution at large rapidities, the BK equation reads

$$\frac{\partial \phi(k)}{\partial y} = \int \frac{dk'^2}{k'^2} \left[\frac{k'^2 \phi(k') - k^2 \phi(k)}{|k'^2 - k^2|} + \frac{k^2 \phi(k)}{\sqrt{4k'^4 + k^4}} \right] - \phi(k)^2, \quad (2)$$

with the reduced rapidity $y = (\alpha_s N_c / \pi) Y$. In this equation α_s is fixed. For $\alpha_s = 0.2$, the maximum $y = 10$ considered in this paper corresponds to large physical rapidities $Y \sim 50$.

The equation is solved using a 4th-order Runge-Kutta algorithm with step $\Delta y =$

0.025. The integral is evaluated in the domain $-15 < \ln k < 35$ using a Gauss-Chebyshev quadrature with 400 points. Henceforth units of transverse momenta will be GeV, with the units corresponding to other quantities to be read from the respective equations. By varying the integration limits, the number of points, the step Δy , and by comparison with previous algorithms [17, 19, 23], the accuracy of the computations can be estimated to be better than 1 % in a wide region excluding one order of magnitude from the limits of the domain. It is usually much better than that. The size of this domain allows us to safely study the evolution up to $y = 10$.

2.1 Initial conditions

We will use Eq. (2) to evolve individual configurations at initial rapidity $y = 0$, characterized by some functional form and by a given value of the saturation scale $Q_{s0} \equiv Q_s(y = 0)$. The first functional form (GBW) essayed is motivated by the Golec-Biernat-Wüsthoff model [45],

$$\phi_{GBW}(k) = -\frac{1}{2} \operatorname{Ei}\left(\frac{k^2}{Q_{s0}^2}\right), \quad (3)$$

with Ei the exponential-integral function. The second functional form (MF) reads

$$\phi_{MF}(k) = \gamma_E + \Gamma(0, \xi) + \ln \xi, \quad \xi = \left(\frac{Q_{s0}^2}{k^2}\right)^\delta, \quad (4)$$

with γ_E the Euler constant and Γ the incomplete gamma function. This form is motivated by phenomenological studies of geometric scaling in γ^* -nucleon and nucleus collisions [34]. It behaves $\propto \xi (\ln \xi)$ for $k \gg (\ll) Q_{s0}$. The parameter δ in this functional form acts as one minus the anomalous dimension governing the behavior of ϕ for large k . We take² $\delta = 1$.

Values of the saturation scale in the region $10^{-2} \leq Q_{s0}^2 \leq 10^2$ have been explored for both initial conditions. This region defines our averaging domain and has been sampled in 284 points which are roughly equidistant in logarithmic scale.

²Initial values $\delta > \delta_c$, $\delta_c = 0.627\dots$, are known [30] to develop a wave front with $\delta = \delta_c$. On the other hand, initial values $\delta < \delta_c$ produce wave fronts which preserve this initial value of δ , a behavior which has been numerically verified in [46] and apparently contradicts previous numerical studies [24]. We have checked that the reason for this apparent contradiction lies in the different regions of transverse momentum studied in both references. The wave front is characterized by the initial value of δ for very large values of k studied in [46] but not considered in [24].

2.2 Averaging procedure and cut-off

After evolving up to a given rapidity y , we compute the average of $\phi(k)$ as proposed in [47] i.e.

$$\langle \phi(k) \rangle_y = \frac{\int_{10^{-2}}^{10^2} dQ_{s0}^2 W(Q_{s0}^2) \phi(k)}{\int_{10^{-2}}^{10^2} dQ_{s0}^2 W(Q_{s0}^2)} \quad (5)$$

is performed. Two different averaging procedures have been considered: the linear averaging [47]

$$W_1(Q_{s0}^2) = \exp \left[-\frac{(Q_{s0}^2 - \langle Q_{s0}^2 \rangle)^2}{\Delta} \right] \quad (6)$$

and the logarithmic averaging procedure given by

$$W_2(Q_{s0}^2) = \frac{1}{Q_{s0}^2} \exp \left[-\frac{(\ln Q_{s0}^2 - \ln \langle Q_{s0}^2 \rangle)^2}{\Delta_l} \right], \quad (7)$$

with $\langle Q_{s0}^2 \rangle = 1$. Values of $\Delta, \Delta_l = 0.01, 0.1, 1, 10$ and 100 have been explored. Let us note that for both for the linear and the logarithmic case, $\Delta, \Delta_l = 0.01$ is almost equivalent to a δ -function, while for $\Delta, \Delta_l = 100$ roughly 50 % of the normalization of the function is contained in the region we study, $10^{-2} \leq Q_{s0}^2 \leq 10^2$. Finally, W_2 with $\Delta_l = 100$ is quite a flat function, with a variation ~ 20 % in the considered region - thus it is our model case for a wide averaging. Let us indicate that although the practical relevance of such large values of Δ, Δ_l may be questionable, our aim in this paper is to examine whether this modification of standard BK evolution has any effect or not - thus our attitude of taking extreme values of the parameters characterizing the width of the weight functions for the averaging.

On the other hand, and following the suggestion about the discreteness of the evolution in [38], see also [46, 48], we have also introduced what we call a cut-off evolution: at every step in the evolution in Eq. (2), values of $\phi(k) < \kappa$ in the r.h.s. of this equation have been set to 0:

$$\begin{aligned} \frac{\partial \phi(k)}{\partial y} &= \int \frac{dk'^2}{k'^2} \left[\frac{k'^2 \phi(k') \theta[\phi(k') - \kappa] - k^2 \phi(k) \theta[\phi(k) - \kappa]}{|k'^2 - k^2|} + \frac{k^2 \phi(k) \theta[\phi(k) - \kappa]}{\sqrt{4k'^4 + k^4}} \right] \\ &- \phi(k)^2 \theta[\phi(k) - \kappa], \end{aligned} \quad (8)$$

with $\theta[x]$ the step function. Values of the cut-off $\kappa = 0.002, 0.01$ and 0.05 have been used, for evolution starting from a given initial condition with $Q_{s0} = \langle Q_{s0} \rangle = 1$. In principle, such cut-off is proportional to the inverse of the coupling constant, but with an unknown proportionality constant which prevents us from making such connection with the value of α_s in the definition of y .

3 Results

We have performed the evolution (2) starting from the initial conditions indicated in Subsection 2.1. In Fig. 1 the evolution for both initial conditions GBW and MF, for 9 given individual configurations with $Q_{s0}^2 = 0.01, 0.04, 0.1, 0.31, 1, 3.31, 10, 30$ and 100, for linear and logarithmic averages, and for the cut-off evolution³, are shown. The development of traveling waves [30] can be seen in all cases and for both initial conditions. For this reason, from now on we will present results only for MF, the results for GBW being in agreement.

In these plots no dramatic effect of the averaging can be observed, the large- k behavior appearing very similar to that of the individual configurations. This fact could be expected from the power-like behavior of the solutions of BK [23, 27, 28, 30] at large k . In order to see the details of the effect of the averaging we show in Fig. 2 a zoom of Fig. 1 (lower-left) in linear vertical scale. The picture shows clearly the mixing of individual configurations performed by the averaging procedure, substantiating for BK evolution the picture in [38]. It can also be seen that the effect of the averaging is more evident in the initial condition and becomes less evident with increasing rapidities.

In the next two Subsections we will examine in more detail two features of evolution, namely the approach to a universal scaling form and the evolution of the saturation scale with rapidity.

³In the curves which result from this cut-off evolution, a discontinuity in the derivative induced by the cut-off is clearly visible.

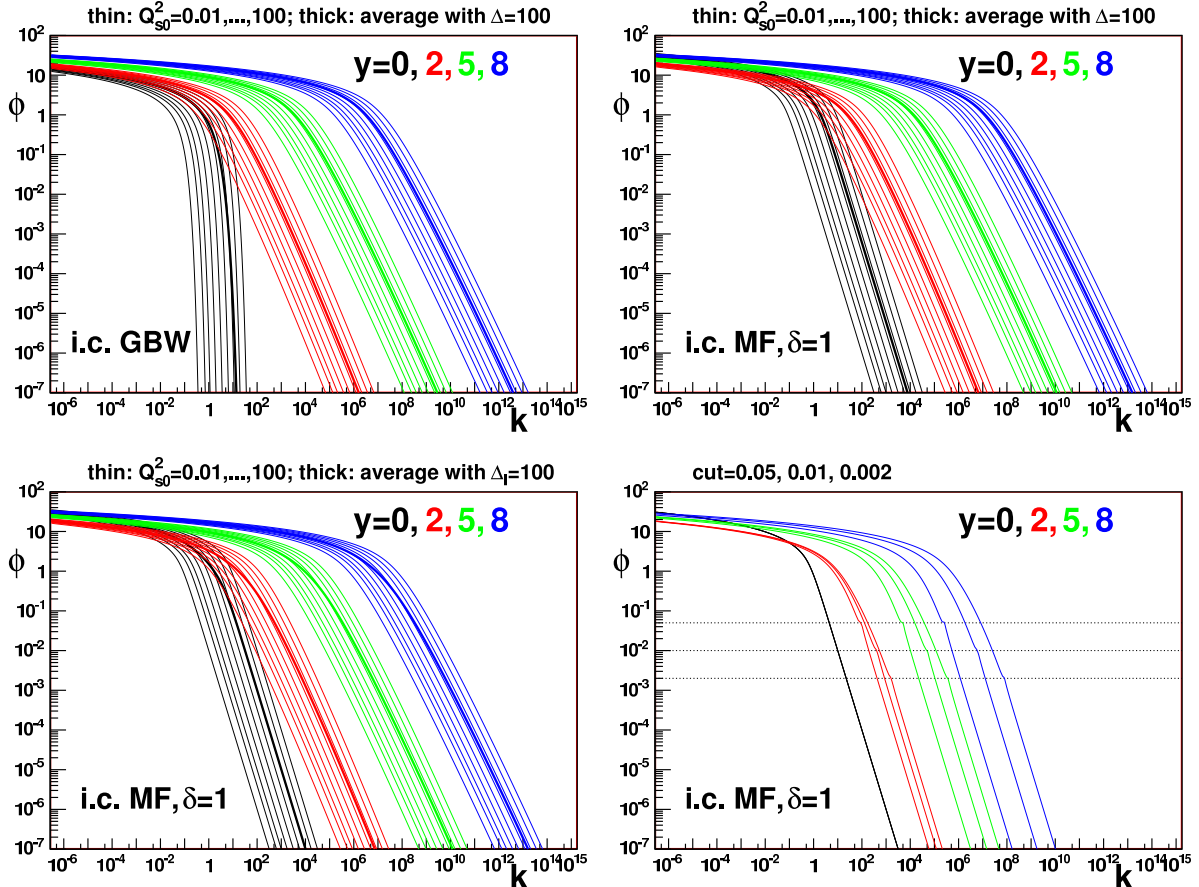


Figure 1: BK evolution starting from GBW (upper-left plot) and MF (the other three plots) initial conditions, both for individual configurations with $Q_{s0}^2 = 0.01, 0.04, 0.1, 0.31, 1, 3.31, 10, 30$ and 100 (thin lines left to right), for linear ($\Delta = 100$, upper plots) and logarithmic averages ($\Delta_l = 100$, lower-left plot) using thick lines, and for cut-off evolution (thin lines, lower-right plot) for (left to right) $\kappa = 0.05, 0.01$ and 0.002 . In this last plot, horizontal dotted lines indicate the values of κ . Results are shown for $y = 0, 2, 5$ and 8 in black, red, green and blue respectively (sets of lines from left to right).

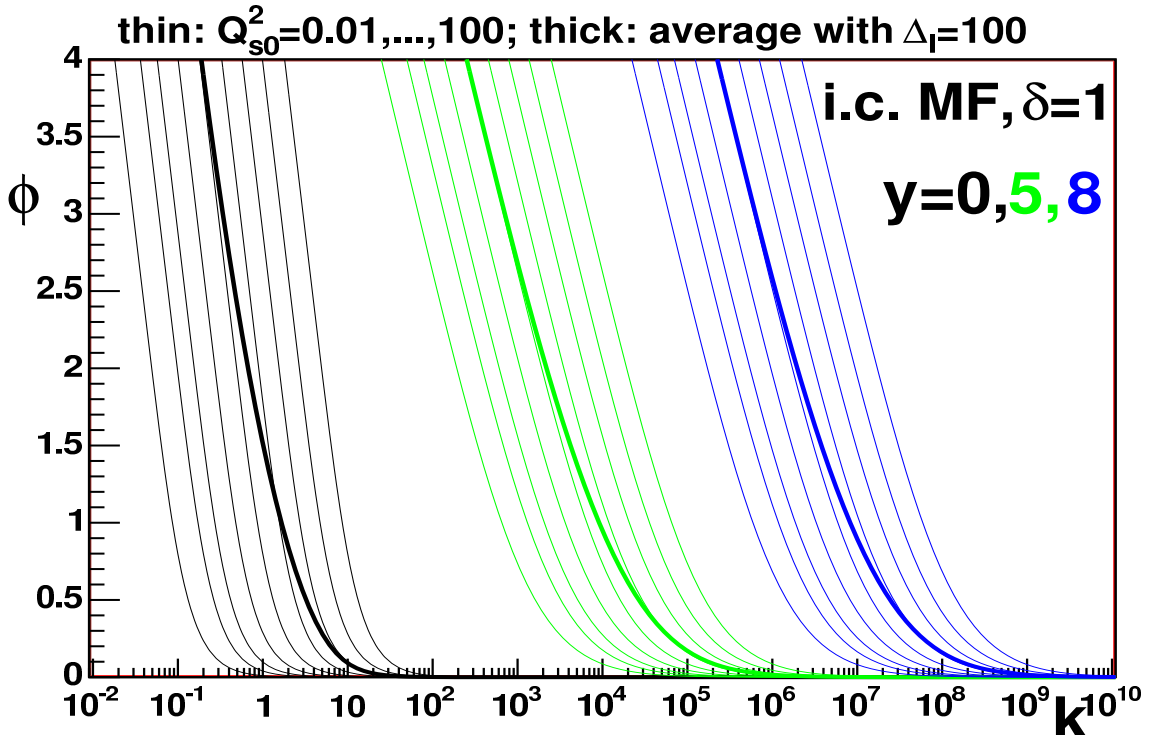


Figure 2: Detail of Fig. 1 (lower-left) in vertical linear scale. Results for $y = 2$ overlap with those for $y = 0$ and are not shown for reasons of clarity.

3.1 Approach to scaling

BK evolution is known [19, 21, 23, 27, 30] to approach asymptotically a scaling function, $\phi(y, k) \rightarrow \phi(k/Q_s(y))$ for $y \rightarrow \infty$, independent of the initial condition for evolution. On the other hand, attempts [37, 38] to go beyond the mean field approximation underlying the BK equation predict a violation of the scaling behavior. Here we try to explore this aspect in order to implement some modifications of BK evolution. In Fig. 3 we show the results for evolution when plotted versus $k/Q_s(y)$, with the saturation scale Q_s determined as discussed in the next Subsection. Curves for an individual configuration with $Q_{s0} = 1$, and for linear and logarithmic averages and for cut-off evolution, are shown. The violation of scaling due to averaging does not look dramatic, the scaling curves being relatively close and getting closer for increasing rapidities. Only the very wide logarithmic averaging with $\Delta_l = 100$ seems to induce some visible violation of scaling, see below. On the other hand, scaling is achieved very quickly in the cut-off evolution (only for the largest cut-off and rapidity some departure is visible). This fact could be expected as it is known [24, 27, 30] that violations of scaling come from the tails of large k , which are cut in the cut-off evolution.

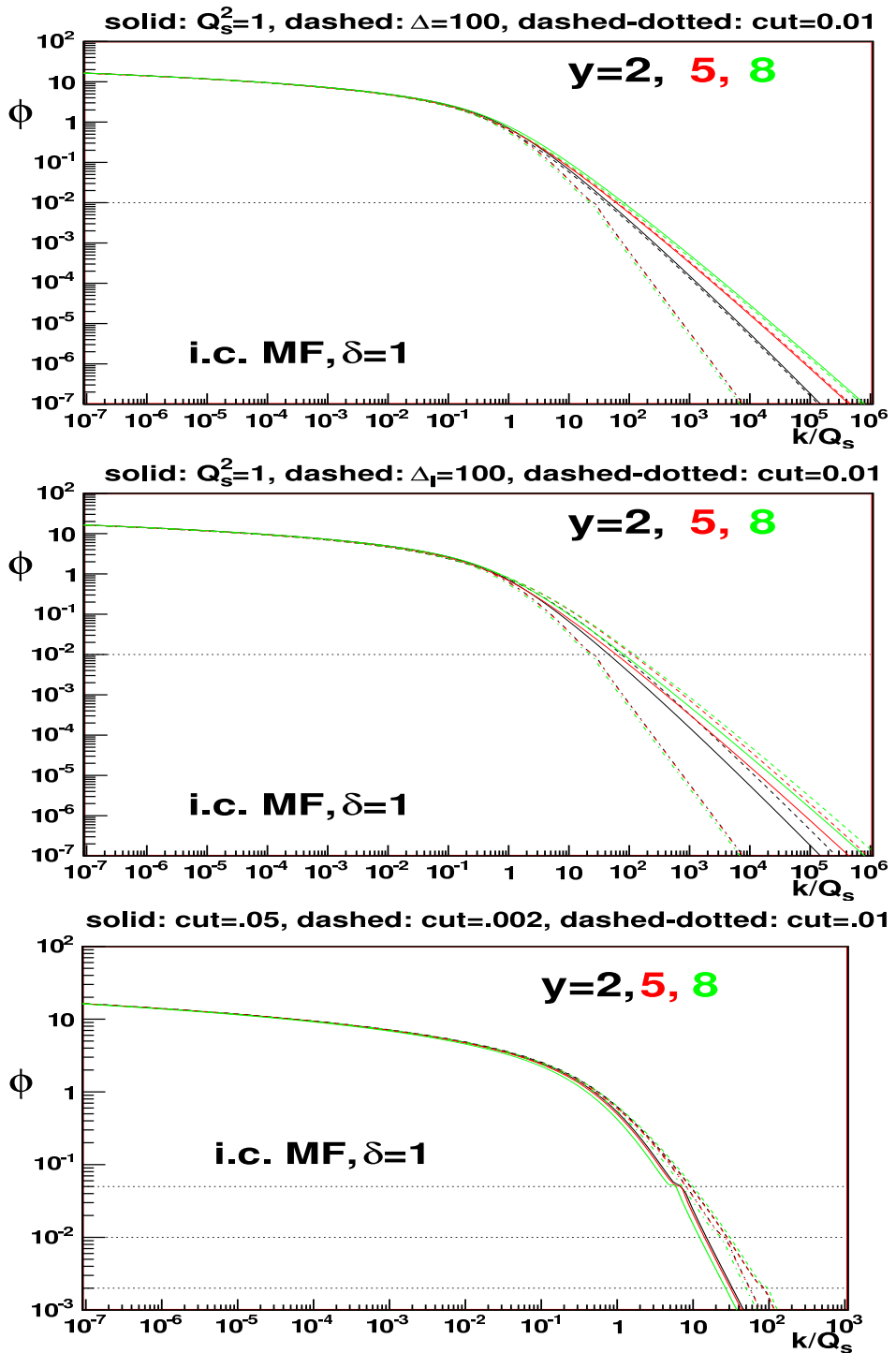


Figure 3: Scaling forms $\phi(k/Q_s(y))$ for evolution starting from MF initial conditions, for $y = 2, 5$ and 8 (black, red and green lines respectively). Upper plot: results of an individual configuration with $Q_{s0} = 1$ (solid lines), of linear ($\Delta = 100$, dashed lines) averaging and with cut-off ($\kappa = 0.01$, dashed-dotted lines). Plot in the middle: idem but for logarithmic ($\Delta_l = 100$) averaging. Lower plot: comparison of the scaling forms for different cut-offs $\kappa = 0.05$ (solid lines), 0.01 (dashed lines) and 0.002 (dashed-dotted lines). In this last plot, horizontal dotted lines indicate the values of κ .

To analyze in more detail the effect of averaging on scaling, in Fig. 4 a zoom of the previous Fig. for the logarithmic averaging is shown. While - as it is well known from standard BK evolution [19,21,23,27,30] - individual configurations quickly tend towards a universal scaling shape for the largest y , the cut-off evolution shows some scaling violation which tends to disappear with increasing $k/Q_s(y)$. Besides, the averaged solutions show a larger violation of scaling than the individual solution at the same y . For example, from the comparison of the curves for rapidities $y = 2, 5, 8$ the violation of scaling induced by the very wide logarithmic averaging with $\Delta_l = 100$ looks ~ 20 % for $k/Q_s(y) = 1$, increasing to ~ 50 % for $k/Q_s(y) = 10$, while the corresponding scaling violations for the individual solutions are noticeably smaller.

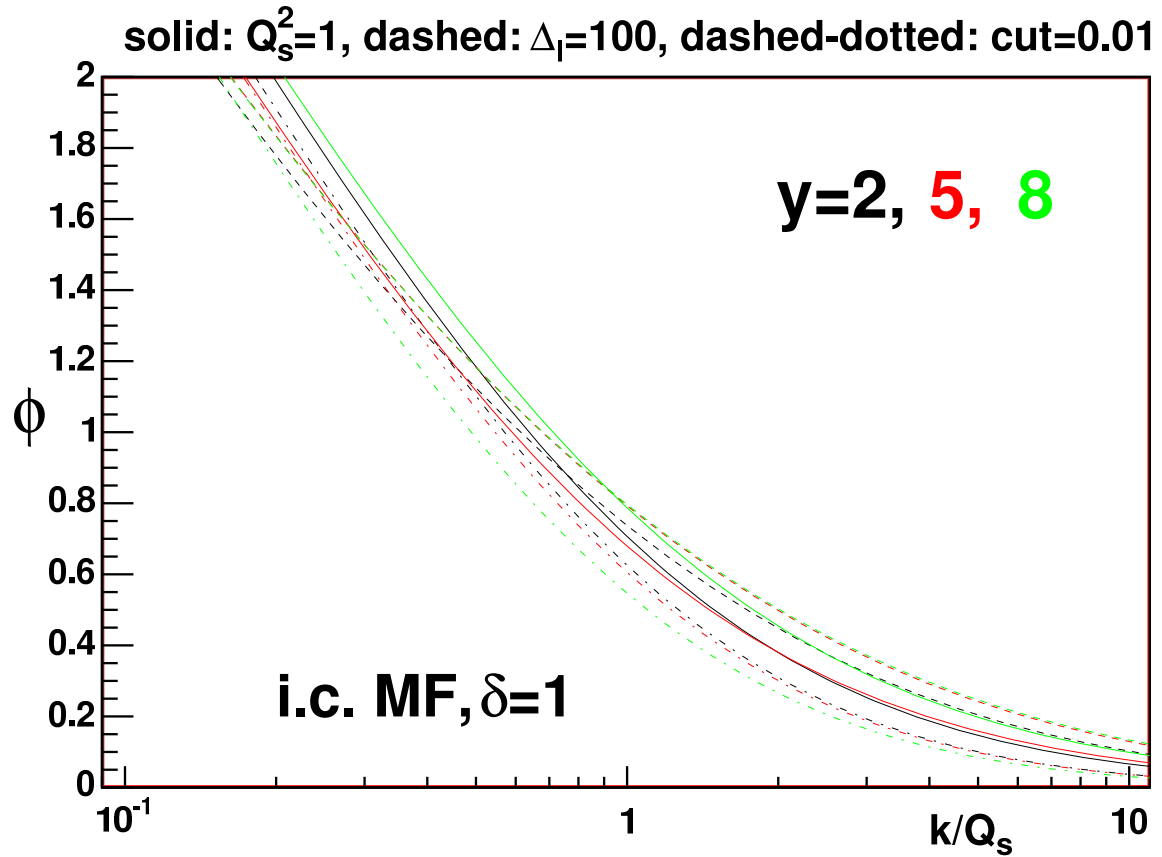


Figure 4: Detail of Fig. 3 (middle) in vertical linear scale, for values of k around $Q_s(y)$.

3.2 Rapidity evolution of the saturation scale

For the function ϕ or the average of individual configurations, obtained by evolution up to a given y , we compute the saturation scale as the position of the maximum of the function $h(k) = k^2 \nabla_k^2 \phi(k)$, as done in previous works [17, 19, 23]⁴. This function shows a Gaussian-like shape which is preserved in the evolution, and the velocity of the evolution with y of this soliton-like form is given by the saturation scale. An error, corresponding to the distance between neighbors in the grid at the saturation scale, is assigned to every value of the saturation scale.

In Fig. 5 we show the results for the evolution of the saturation scale with reduced rapidity y . In order to quantify eventual differences, we have performed a fit to an exponential form⁵ $Q_s^2(y) = ce^{dy}$ in the region $3 < y < 9$.

The averaging procedure shows no sizable effect, a fact which can be easily understood as BK evolution is known [19, 21, 23, 27, 30] to lead asymptotically to a universal wave front moving with universal velocity (for ‘supercritical’ initial conditions, see the footnote in Subsection 2.1). Thus, asymptotically every individual configuration (even those arising from initial conditions not only with different initial saturation scale but also with different functional shape) will move with the same velocity, and the average will be characterized by this common velocity.

On the other hand, the cut-off evolution shows a strong influence on the y -evolution of the saturation scale: the larger the value of the cut-off parameter κ , the slower the evolution. This corresponds to the fact that the evolution is driven [23, 27, 30] by the large- k regions, as discussed previously in Subsection 3.1.

⁴Note that this choice corresponds to a region where the function is large, $\phi \sim 1$, and not to a dilute region of the traveling wave. It is known [24, 46, 49] that with this definition, sub-leading terms [32] are less noticeable. In any case, we do not attempt to study in detail the behavior of the saturation scale with rapidity but only to see whether clear differences among the different modifications of BK evolution appear or not.

⁵The value of d expected [27, 28, 30] is $d \simeq 4.88$; for evolution of individual configurations and for the average, we get a smaller value, $d \simeq 4.45$, due to the neglected sub-leading terms [24, 32, 46, 49] in the y -behavior of the saturation scale.

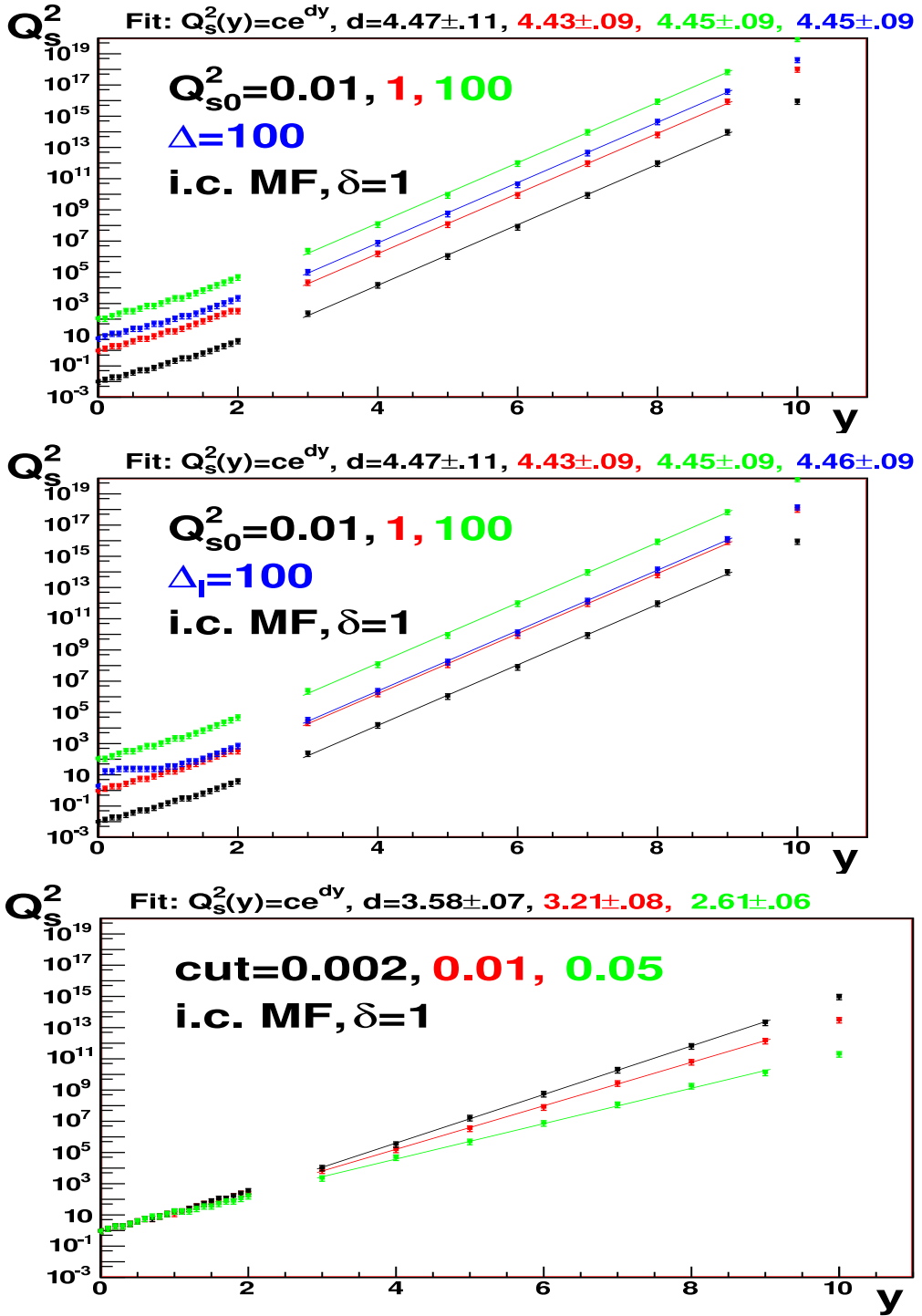


Figure 5: Q_s^2 versus y for evolution starting from MF initial conditions. In the upper and middle plots, the results for the evolution of individual configurations are shown for $Q_{s0}^2 = 0.01, 1$ and 100 in black, red and green respectively, while in blue the results for linear ($\Delta = 100$, upper plot) and logarithmic ($\Delta_l = 100$, middle plot) are presented. In the lower plot, results of the cut-off evolution for $\kappa = 0.002$ (black), 0.01 (red) and 0.05 (green) are presented. In the plots, straight lines correspond to fits to $Q_s^2(y) = ce^{dy}$ in the region $3 < y < 9$, with the values of d indicated in the plots.

Other interesting quantity which we can examine⁶ is not the saturation scale of the averaged solution, but the average saturation scale. In the language of [30–32], the evolution of the saturation scale with rapidity shows the speed of the wave front in its movement towards higher transverse momenta. Thus the dispersion of the saturation scale at a given rapidity will reflect the spread of the ensemble of wave fronts coming through evolution from a given ensemble of initial conditions.

We define the average of any observable $\langle \mathcal{O}(y) \rangle$ by substituting $\phi(k)$ by $\mathcal{O}(y)$ in Eq. (5). In Fig. 6 we plot the average values $\langle Q_s^2(y) \rangle$ and $\langle \ln Q_s^2(y) \rangle$ and the corresponding dispersions, versus rapidity, for linear and logarithmic weight functions and two different values of Δ, Δ_l . Both the average $Q_s^2(y)$ and its dispersion show the same dependence with y , so the width of the ensemble of wave fronts gets wider and wider with increasing rapidity. On the other hand, the dispersion of $\ln Q_s^2(y)$ stays constant (within our numerical accuracy) during evolution - a behavior opposite to the linear y -dependence found in discrete evolution [38, 46]. Besides, smaller initial widths result in smaller widths after evolution. We expect these characteristics to remain true for large enough rapidity even if the weight functions for averaging are more involved, or even for initial ensembles containing different shapes. This is due to the fact that BK evolution eventually leads to a universal shape which, once roughly built, will evolve with the characteristics we have discussed.

4 Discussion

Much theoretical effort has been directed recently to go beyond the standard JIMWLK framework to study the small- x structure of hadrons: the role of correlations [36, 38, 47, 50–52], of discreteness in gluon emissions [38, 53] and the relevance of Pomeron loops [37, 39–44, 54–59]. Numerical studies are just starting [25, 46, 48, 60].

In this paper we contribute to this subject through an attempt to quantify numerically the relevance of two of these aspects, namely correlations through averaging [47] and discreteness of gluon emissions [38], on standard BK evolution. The averaging of individual configurations results in scaling violations, but their size around the saturation scale is not dramatically large. On the other hand, the evolution of the saturation

⁶We thank Alex Kovner for drawing our attention on this point.

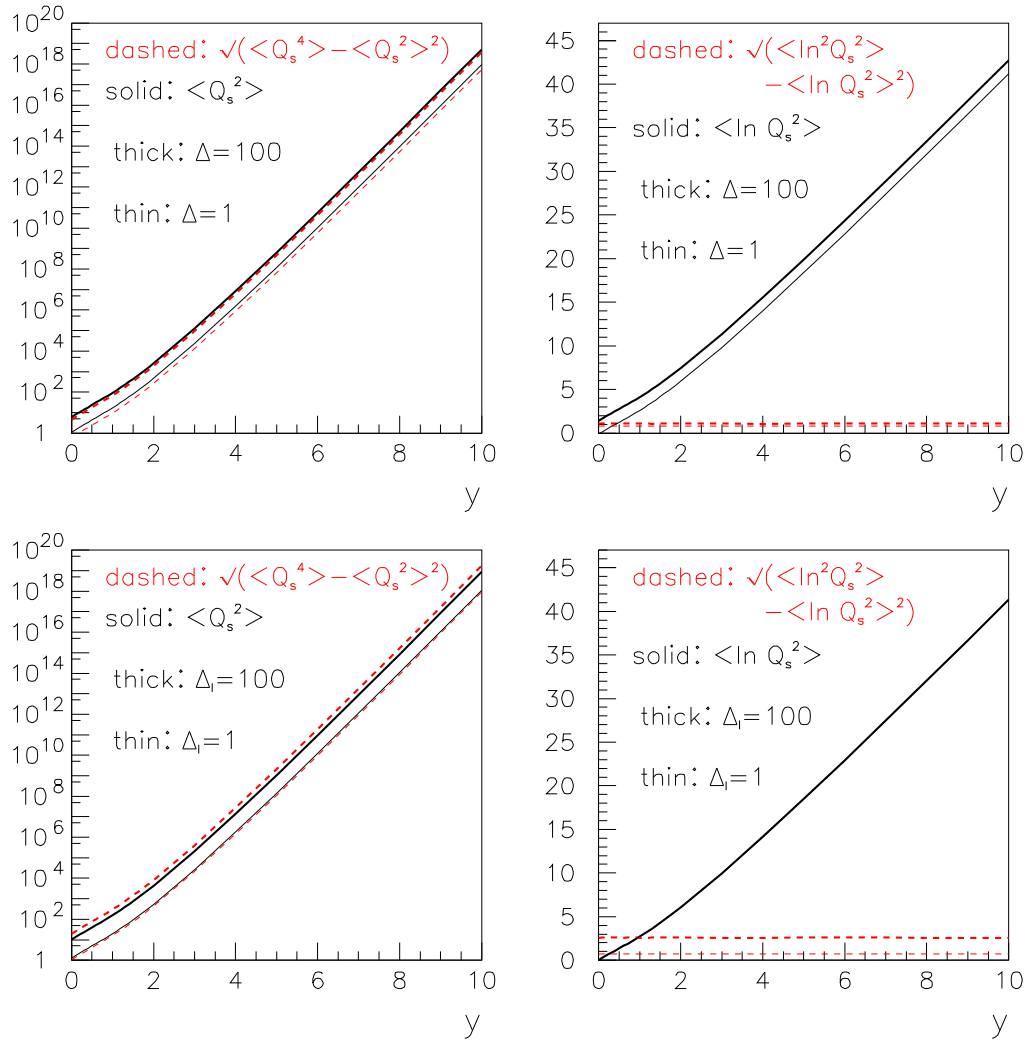


Figure 6: $\langle Q_s^2(y) \rangle$ (black solid lines in the plots on the left), $\langle \ln Q_s^2(y) \rangle$ (black solid lines in the plots on the right), and their corresponding dispersions (red dashed lines in the plots on the left and right respectively) versus y , for linear (upper plots) and Gaussian (lower plots) averaging with $\Delta, \Delta_l = 100$ (thick lines) and 1 (thin lines), for evolution starting from MF initial conditions. The difference between thick and thin red dashed lines in the upper-right plot, and between thick and thin black solid lines in the lower-right plot, is numerically very small and hardly visible.

scale with rapidity, and the large- k behavior of the solutions, seem to be hardly affected. Finally, the dispersion in the saturation scale of the individual solutions increases with rapidity as fast as the corresponding average, indicating that the width of the ensemble of evolved solutions gets wider and wider with increasing rapidity.

The implementation of discreteness in the evolution through a cut-off does not alter strongly the scaling properties. On the other hand, the saturation scale evolves slower with rapidity with increasing value of the cut-off, and the solutions at large k become steeper, than in the standard BK evolution.

In view of the differences among the effects of different modifications on standard BK evolution, of the fact that the experimentally accessible regions of Y are pre-asymptotic and dominated by the initial conditions [24, 34, 35], and of the additional uncertainties on the form of the averaging weight function and/or size of the cut-off, any claim on phenomenological implications of our study looks premature. Besides, our implementation of these modifications of BK evolution is simplistic, so their results can only be taken as hints of the possible effects of a proper application of such modifications. Nevertheless, we find their effects large enough to justify the further investigations, both on the analytical and on the numerical side, currently under development to rigorously develop and implement all these new ideas.

Acknowledgments: We thank M. A. Braun, E. Iancu, J. Jalilian-Marian, A. H. Mueller and U. A. Wiedemann for useful discussions. Special thanks are given to J. L. Albacete, A. Kovner and M. Lublinsky for many fruitful discussions and suggestions, and a critical reading of the manuscript. N.A. acknowledges financial support of Ministerio de Educación y Ciencia of Spain under a contract Ramón y Cajal, and of CICYT of Spain under project FPA2002-01161. J.G.M. acknowledges the partial financial support from the Fundação para a Ciência e a Tecnologia of Portugal under contract SFRH/BPD/12112/2003. N.A. also thanks IST, and J.G.M. Departamento de Física de Partículas at the Universidade de Santiago de Compostela, for warm hospitality while part of this work was done.

References

- [1] L. D. McLerran and R. Venugopalan, Phys. Rev. D **49**, 2233 (1994).
- [2] L. D. McLerran and R. Venugopalan, Phys. Rev. D **49**, 3352 (1994).
- [3] L. D. McLerran and R. Venugopalan, Phys. Rev. D **50**, 2225 (1994).

- [4] J. Jalilian-Marian, A. Kovner, L. D. McLerran and H. Weigert, Phys. Rev. D **55**, 5414 (1997).
- [5] J. Jalilian-Marian, A. Kovner, A. Leonidov and H. Weigert, Phys. Rev. D **59**, 014014 (1999).
- [6] J. Jalilian-Marian, A. Kovner and H. Weigert, Phys. Rev. D **59**, 014015 (1999).
- [7] A. Kovner and J. G. Milhano, Phys. Rev. D **61**, 014012 (2000).
- [8] A. Kovner, J. G. Milhano and H. Weigert, Phys. Rev. D **62**, 114005 (2000).
- [9] E. Iancu, A. Leonidov and L. D. McLerran, Nucl. Phys. A **692**, 583 (2001).
- [10] E. Iancu, A. Leonidov and L. D. McLerran, Phys. Lett. B **510**, 133 (2001).
- [11] E. Ferreiro, E. Iancu, A. Leonidov and L. McLerran, Nucl. Phys. A **703**, 489 (2002).
- [12] I. Balitsky, Nucl. Phys. B **463**, 99 (1996).
- [13] A. H. Mueller, Phys. Lett. B **523**, 243 (2001).
- [14] J. P. Blaizot, E. Iancu and H. Weigert, Nucl. Phys. A **713**, 441 (2003).
- [15] H. Weigert, Nucl. Phys. A **703**, 823 (2002).
- [16] L. V. Gribov, E. M. Levin and M. G. Ryskin, Phys. Rept. **100**, 1 (1983).
- [17] M. Braun, Eur. Phys. J. C **16**, 337 (2000).
- [18] M. A. Kimber, J. Kwiecinski and A. D. Martin, Phys. Lett. B **508**, 58 (2001).
- [19] N. Armesto and M. A. Braun, Eur. Phys. J. C **20**, 517 (2001).
- [20] E. Levin and M. Lublinsky, Nucl. Phys. A **696**, 833 (2001).
- [21] M. Lublinsky, Eur. Phys. J. C **21**, 513 (2001).
- [22] K. Golec-Biernat, L. Motyka and A. M. Stasto, Phys. Rev. D **65**, 074037 (2002).
- [23] J. L. Albacete, N. Armesto, A. Kovner, C. A. Salgado and U. A. Wiedemann, Phys. Rev. Lett. **92**, 082001 (2004).

- [24] J. L. Albacete, N. Armesto, J. G. Milhano, C. A. Salgado and U. A. Wiedemann, Phys. Rev. D **71**, 014003 (2005).
- [25] K. Rummukainen and H. Weigert, Nucl. Phys. A **739**, 183 (2004).
- [26] E. Levin and K. Tuchin, Nucl. Phys. B **573**, 833 (2000).
- [27] E. Iancu, K. Itakura and L. McLerran, Nucl. Phys. A **708**, 327 (2002).
- [28] A. H. Mueller and D. N. Triantafyllopoulos, Nucl. Phys. B **640**, 331 (2002).
- [29] A. H. Mueller, Nucl. Phys. A **724**, 223 (2003).
- [30] S. Munier and R. Peschanski, Phys. Rev. Lett. **91**, 232001 (2003).
- [31] S. Munier and R. Peschanski, Phys. Rev. D **69**, 034008 (2004).
- [32] S. Munier and R. Peschanski, Phys. Rev. D **70**, 077503 (2004).
- [33] Y. V. Kovchegov, Phys. Rev. D **60**, 034008 (1999).
- [34] N. Armesto, C. A. Salgado and U. A. Wiedemann, Phys. Rev. Lett. **94**, 022002 (2005).
- [35] J. L. Albacete, N. Armesto, J. G. Milhano, C. A. Salgado and U. A. Wiedemann, Eur. Phys. J. C **43**, 353 (2005).
- [36] E. Levin and M. Lublinsky, Nucl. Phys. A **730**, 191 (2004).
- [37] A. H. Mueller and A. I. Shoshi, Nucl. Phys. B **692**, 175 (2004).
- [38] E. Iancu, A. H. Mueller and S. Munier, Phys. Lett. B **606**, 342 (2005).
- [39] E. Iancu and D. N. Triantafyllopoulos, Nucl. Phys. A **756**, 419 (2005).
- [40] A. H. Mueller, A. I. Shoshi and S. M. H. Wong, Nucl. Phys. B **715**, 440 (2005).
- [41] E. Levin and M. Lublinsky, Nucl. Phys. A **763**, 172 (2005).
- [42] E. Iancu and D. N. Triantafyllopoulos, Phys. Lett. B **610**, 253 (2005).
- [43] A. Kovner and M. Lublinsky, Phys. Rev. Lett. **94**, 181603 (2005).
- [44] A. Kovner and M. Lublinsky, Phys. Rev. D **72**, 074023 (2005).

- [45] K. Golec-Biernat and M. Wusthoff, Phys. Rev. D **59**, 014017 (1999).
- [46] R. Enberg, K. Golec-Biernat and S. Munier, Phys. Rev. D **72**, 074021 (2005).
- [47] A. Kovner and M. Lublinsky, JHEP **0503**, 001 (2005).
- [48] G. Soyez, Phys. Rev. D **72**, 016007 (2005).
- [49] K. Golec-Biernat, arXiv:hep-ph/0408255.
- [50] R. A. Janik, arXiv:hep-ph/0409256.
- [51] E. Levin and M. Lublinsky, Phys. Lett. B **607**, 131 (2005).
- [52] C. Marquet, R. Peschanski and G. Soyez, arXiv:hep-ph/0512186.
- [53] G. P. Salam, Nucl. Phys. B **461**, 512 (1996).
- [54] A. Kovner and M. Lublinsky, Phys. Rev. D **71**, 085004 (2005).
- [55] J. P. Blaizot, E. Iancu, K. Itakura and D. N. Triantafyllopoulos, Phys. Lett. B **615**, 221 (2005).
- [56] Y. Hatta, E. Iancu, L. McLerran and A. Stasto, Nucl. Phys. A **762**, 272 (2005).
- [57] Y. Hatta, E. Iancu, L. McLerran, A. Stasto and D. N. Triantafyllopoulos, arXiv:hep-ph/0504182.
- [58] A. I. Shoshi and B. W. Xiao, arXiv:hep-ph/0512206.
- [59] E. Iancu, G. Soyez and D. N. Triantafyllopoulos, arXiv:hep-ph/0510094.
- [60] V. A. Abramovsky and N. V. Prikhod'ko, arXiv:hep-ph/0512343.